Water Tunnel Turbulence Measurements Behind a Honeycomb

Basil E. Robbins*
The Pennsylvania State University, State College, Pa.

The results of turbulence measurements made in a 48-in. (1.22-m) diam water tunnel with and without an upstream honeycomb are reported. Comparison is made to previous measurements made behind a similar honeycomb. Axial turbulence intensity measurements agreed well with previously predicted levels in the test section, as well as this author's predicted levels based on plenum section measurements. In addition, the longitudinal integral length scale was estimated in the test section. Spectral analysis showed an abnormally high turbulent energy level at low flow speeds; higher flow velocities had energy spectra with consistently lower levels and similar shapes. Recommendations are given for the tunnel operating conditions that produce minimum turbulence levels.

Nomenclature

A = constant, intercept of the hot-film calibration curve
B = slope of the hot-film calibration curve
$\bar{E}$ = mean or dc component of the anemometer bridge voltage
F = normalized spectral density of the kinetic energy per unit mass defined in Eq. (8)
Re = Reynolds number
$\bar{U}$ = mean flow velocity
c = speed of sound
d = 4.0 in. (10.16 cm)—cell size of the large honeycomb; 0.22 in. (0.56 cm)—cell size of the small honeycomb
e = fluctuating or ac component of the anemometer bridge voltage
f = frequency
n = constant
p' = acoustic pressure amplitude
u = fluctuating or turbulent velocity
x = distance downstream from the honeycomb
Λ_L = longitudinal integral length scale
Λ_τ = temporal integral scale
ν = kinematic viscosity
ρ = density
$\rho(\tau)$ = autocorrelation coefficient
τ = time delay

Subscripts

P = plenum section
T = test section

Introduction

THE need for low freestream turbulence levels in water tunnels has increased over the last few years. With advancements in underwater body design, in the use of boundary-layer control methods, and in the design of improved propulsion systems, the desire to improve drag performance through laminarization of the body boundary layer has greatly increased. In ordinary tunnels, the interpretation of results and their application to design is complicated if turbulence effects are present, i.e., it is difficult to separate the effects of both Reynolds number and turbulence. In order to study the effects of turbulence, it is often desirable to be able to vary the degree of turbulence in the tunnel. It is, therefore, important to know the initial or background turbulence level and its characteristics; the turbulence characteristics created behind a grid could be influenced by the initial turbulence upstream of the grid.

Received Aug. 29, 1977; revision received Feb. 17, 1978.

Index category: Hydrodynamics.

*Research Assistant, Applied Research Laboratory. Member AIAA.

In August of 1964, an aluminum honeycomb was installed in the settling section of the 48-in. (1.22-m) diam water tunnel of the Garfield Thomas Water Tunnel at the Applied Research Laboratory on the campus of The Pennsylvania State University for the purpose of turbulence reduction. Initial measurements were taken in March 1965 after the installation of the honeycomb. In March 1966, measurements were again made behind the honeycomb. The deterioration was so extensive that the honeycomb was finally removed in March 1966.

The measurements described in this paper were made before and after the installation of a stainless steel honeycomb in the settling section; the hexagonal cells are 18.75 in. (47.62 cm) long and 0.22 in. (0.56 cm) across the flats. The honeycomb was manufactured by Honeycomb Corporation of America located in Bridgeport, Conn. A comparison is made between the theory described in Lumley and McMahon's paper [1] and these latest measurements. In addition, a comparison is made between predicted test section levels from plenum section measurements and test section measurements.

Instrumentation

The characteristics of the turbulent flow were measured with both a parabolic and a conical hot-film probe mounted on a strut in the test section and in the plenum section. The parabolic probe was used in the test prior to the installation of the honeycomb. The same mounting strut was used in both the test section and plenum section. The probe mounting strut was bolted to the test section floor; the probe was positioned 14.25 in. (36.20 cm) from the test section wall. The probe holder was physically attached to the strut by a bolt and nut arrangement. In addition, an accelerometer was mounted inside the strut end cap to detect transverse strut vibrations. As a point of interest, during the test there were no vibratory signals discernible above the background electrical noise. The electrical leads were brought out of the tunnel balance box through a passageway inside the strut. The strut was sealed with RTV and the surface indentations (bolt holes) filled with candle wax. After the installation of the honeycomb, an inspection of the parabolic probe revealed it had a small crack in its quartz coating, so a conical probe was used in its place. The same mounting strut was used again in the test section. However, the probe support was epoxied to the end cap to prevent water leakage.

A sealing problem occurred in the probe support and caused a short circuit. This caused the electrical signals to become spiky; they appeared intermittently and with varying levels of amplitude. When a new probe support was used and completely sealed with epoxy the electrical problems ended.

The electronics were set up to make sequential readings of the mean axial velocity, axial turbulence intensity, axial component of the turbulent energy spectrum, and to record

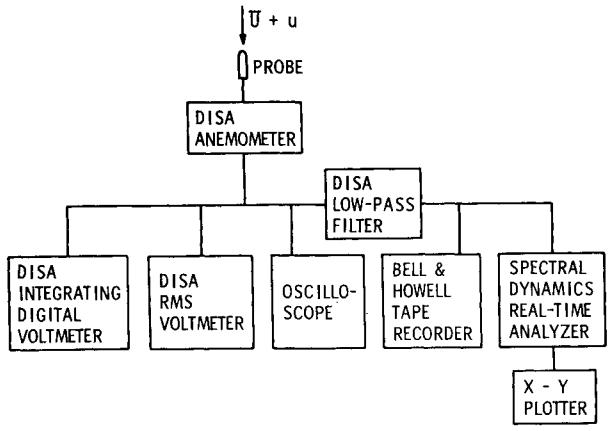

Fig. 1 Basic mean velocity and turbulence intensity equipment setup.

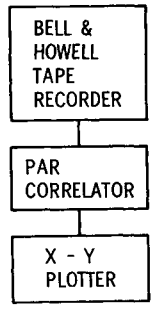

Fig. 2 Instrumentation for determination of auto-correlation coefficient.

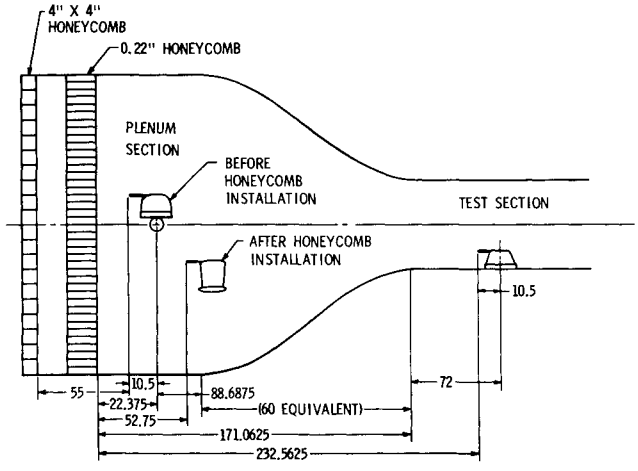

Fig. 3 Diagram of the probe positions within the 48-in. water tunnel.

the anemometer signal for later determination of the integral length scale. A block diagram of the electronic equipment setup is shown in Fig. 1. One of the sensing elements was a Thermo-Systems parabolic hot-film probe, model 1235K-W. Its frequency response is 70,000 Hz per Thermo-Systems probe manual. The second probe was a Thermo-Systems conical hot-film probe, model 1230N-W. Its frequency response is stated to be flat to 3000 Hz. These probes were powered by a DISA model 55M10 anemometer. The dc part of the anemometer signal was integrated for 30 s by a DISA digital voltmeter. These readings are proportional to the axial mean velocity and were used to generate a calibration curve. A DISA rms voltmeter was used to obtain the axial turbulence intensity by integrating for 30 s; the rms level of the ac part of the signal is in direct proportion to the turbulence intensity. During the tests, an oscilloscope was used to monitor the anemometer signal. A low-pass filter cut off the anemometer signal above 50,000 Hz, which was connected to a Bell & Howell magnetic tape recorder and a Spectral Dynamics Corp. SD-301C real time analyzer. The tape recorder was used to store the data for later autocorrelation analysis to determine the longitudinal integral length scale. A frequency spectrum was made at each flow condition on the real time analyzer at the time the turbulence and mean flow measurements were being made.

Later, the taped signal was played back through a Princeton Applied Research (PAR) correlator, model 101 to obtain a graph of the autocorrelation coefficient on an *x-y* plotter. This setup is schematically shown in Fig. 2. Then, this autocorrelation function was integrated to obtain the longitudinal integral length scale.

Data Acquisition

Mean Velocity

The heat transfer from the parabolic and conical hot-film probes was approximated by King's law derived for a circular cylinder. In these tests, the tunnel flow velocity was known and controlled, so the following expression was used to define the calibration curve during the tests:

$$\bar{E}^2 = A + B\bar{U}^{1/n} \tag{1}$$

where $\bar{E}$ is the dc component of the anemometer bridge voltage, A represents the intercept of the calibration curve, B is the slope of that curve, $\bar{U}$ denotes the mean axial velocity, and n is a constant chosen to have its usual value of 2.0.

Turbulence Intensity

Measurement of Test Section Values

The expression for determining the turbulence intensity was derived from King's law by including the fluctuating velocity and electrical components and is given as

$$\frac{\sqrt{\overline{u^2}}}{\bar{U}} = \frac{4\bar{E}\sqrt{\overline{e^2}}}{B\bar{U}^{1/2}} \tag{2}$$

where u represents the fluctuating or turbulent axial velocity component and e is the fluctuating ac voltage from the anemometer bridge circuit. A computerized data reduction program, using Eqs. (1) and (2), was used during the tests. Equation (1) provided the value of B used in Eq. (2) for the turbulence intensity.

Prediction of Test Section Values from Plenum Measurements

The turbulence level in the test section is of greatest importance; however, this is usually difficult to measure due to the low signal-to-electronic noise ratio. In order to obtain a higher signal level, it is necessary to make measurements in the plenum section where the turbulence intensity is higher. These results are then adjusted to the test section by accounting for the effects of turbulence decay length and nozzle contraction.

The effect of decay length accounts for the dissipation of turbulent energy downstream of the honeycomb. The cylindrical plenum section downstream of the honeycomb is approximately 111 in. (2.82 m) long (see Fig. 3). This is followed by a 15 ft (4.57 m) long nozzle with a 9:1 contraction ratio. For an idealized conical nozzle, the equivalent straight section is one-third the length or 5 ft (1.52 m). Thus, the total equivalent length of 171 in. (4.34 m) is available for turbulence decay. The probe in the plenum section was located 52.8 in. (1.34 m) downstream of the honeycomb. Therefore, the ratio of the turbulent velocities in the test section to that in the plenum section is given by

$$\frac{(\overline{u^2})_T}{(\overline{u^2})_P} = \frac{x_P}{x_T} = \frac{52.8}{171} = 0.308 \tag{3}$$

where x represents the distance downstream from the honeycomb, the subscript T indicates test section values, and the subscript P indicates plenum section values.

The effect of nozzle contraction on turbulence is due partly to the elongation of the eddies along the tunnel axis with corresponding contraction in perpendicular directions, and partly to the readjustment of the turbulent velocity components which takes place when the normal isotropic condition is upset. From Lumley and McMahon,[1] for this particular water tunnel, the turbulence intensity in the test section due to contraction can be related to that in the plenum section by the expression

$$\left(\frac{\overline{u^2}}{\bar{U}^2}\right)_T = 0.0516\left(\frac{\overline{u^2}}{\bar{U}^2}\right)_P \tag{4}$$

Combining Eqs. (3) and (4), we can obtain both the effect of decay length and nozzle contraction:

$$\left(\frac{\overline{u^2}}{\bar{U}^2}\right)_T = 0.0516\frac{(\overline{u^2})_T}{(\overline{u^2})_P}\left(\frac{\overline{u^2}}{\bar{U}^2}\right)_P = 0.0159\left(\frac{\overline{u^2}}{\bar{U}^2}\right)_P \tag{5}$$

Now, taking the square root of both sides of Eq. (5), we have

$$\left(\frac{\sqrt{\overline{u^2}}}{\bar{U}}\right)_T = 0.126\left(\frac{\sqrt{\overline{u^2}}}{\bar{U}}\right)_P \tag{6}$$

This expression was derived solely for the flow behind a honeycomb; without the honeycomb, the decay would have to be derived differently because the length scales are different.

Longitudinal Integral Length Scale

The longitudinal or axial integral length scale of the turbulence was estimated from the autocorrelation coefficient, $\rho(\tau)$. This function was obtained by playing back tapes of the turbulent signal through a PAR correlator and recording the correlagram on an x-y plotter.

Integration under the curve of this coefficient yields the temporal integral scale, Λ_τ. In this test, the integration was done by a planimeter. The longitudinal integral length scale, Λ_L, is related to this time scale by the expression

$$\Lambda_L = \bar{U}\Lambda_\tau \tag{7}$$

provided the turbulent eddies are convected downstream at the mean velocity, $\bar{U}$.

The temporal integral scale is a measure of the time in which a typical velocity fluctuation is dependent upon itself and its past history. This would roughly correspond to the time it takes a characteristic turbulent eddy to pass by a fixed point. Similarly, the longitudinal integral length scale is a rough measure of the size of a characteristic turbulent eddy being convected with the flows.

Energy Spectrum

The energy spectrum of the axial component of the turbulence was determined using the instrumentation setup as shown in Fig. 1. A Spectral Dynamics Corp. real time analyzer computed the narrow-band energy spectra. This device sweeps through the frequency bands, computes the spectrum, and displays the results on a cathode-ray tube. Then, on command, the spectrum is graphed on an x-y plotter.

Test Procedure

Since the probe was rigidly mounted, there was no involvement in traversing the flowfield; the only variations in flow conditions were due to controlled tunnel parameters. Three parameters were varied during the first part of the tests—the flow velocity, the tunnel pressure, and the pitch angle of the tunnel drive impeller. The flow velocity was varied from 20 f/s (6.10 m/s) to 60 f/s (18.29 m/s) in 5 f/s (1.52 m/s) increments. The tunnel pressure was held constant at 20 or 28 psia to prevent cavitation of the impeller at the different rotational speeds and pitch settings. The impeller pitch angles were set at 14, 18, and 22.5 deg.

The tests were conducted by setting the pitch angle and tunnel pressure, then increasing the tunnel speed from 20 f/s (6.10 m/s) to 60 f/s (18.29 m/s). At each condition, the mean velocity, turbulence intensity, and energy spectrum were measured, and data tape recordings of the analog signal were taken.

In the tests after the installation of the honeycomb, the impeller pitch angle was set at 22.5 deg. This was found to be the most favorable pitch angle from the first part of the tests prior to the installation of the honeycomb.

Results

Turbulence Intensity

The results of the plenum section measurements are shown in Fig. 4. Here, the turbulence intensity is compared between the no-honeycomb condition and with the honeycomb installed. As shown, for a 22.5-deg impeller pitch angle, the intensity level is reduced as much as 5.5%. These two data sets indicate that the flow regimes are quite different. Without the honeycomb, the flow in the plenum is quite turbulent and the trend in the intensity is to increase with increasing mean flow velocity. Lumley and McMahon[1] found the intensity to decrease with increasing velocity. However, the results from their test section measurements indicate that the intensity increases with increasing velocity; they were unable to explain this discrepancy in trend with probe position and inferred that their probe support vibrated when installed in the test section.

The effect of impeller pitch angle on the intensity in the plenum section appears to be minimal. Figure 4 shows data for both 22.5 and 18 deg, as well as averaged values at a constant flow velocity. These data seem to be consistent, since the intensity levels were nearly the same when some

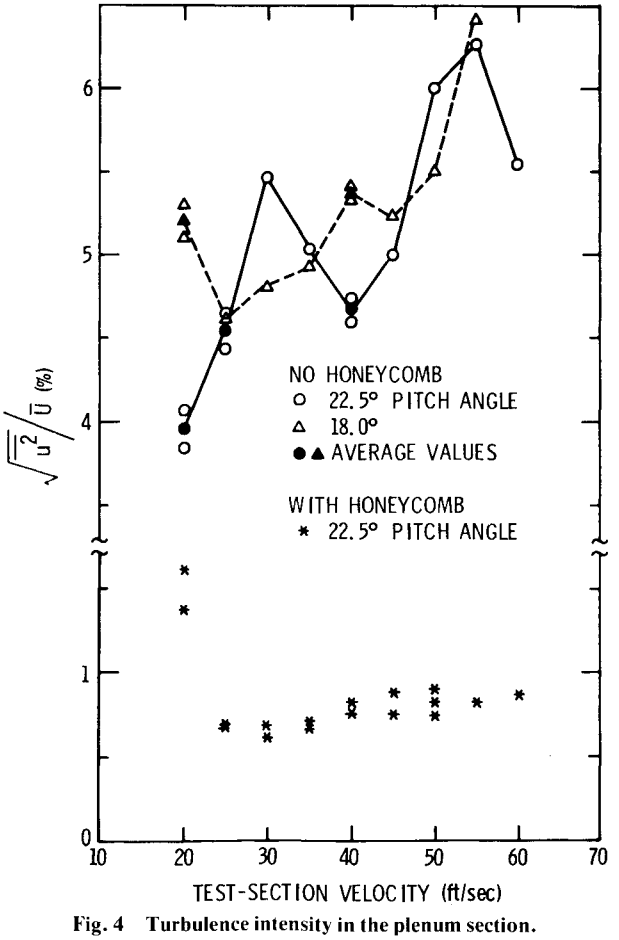

Fig. 4 Turbulence intensity in the plenum section.

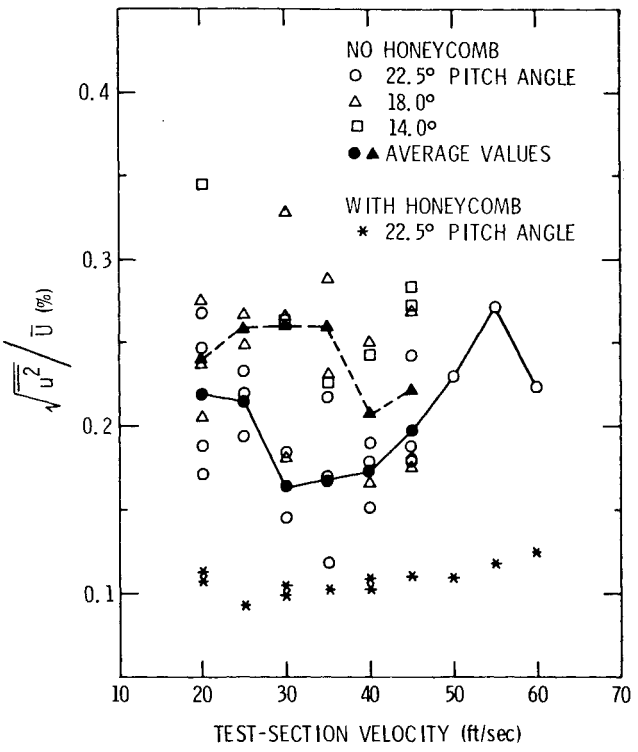

Fig. 5 Turbulence intensity in the test section.

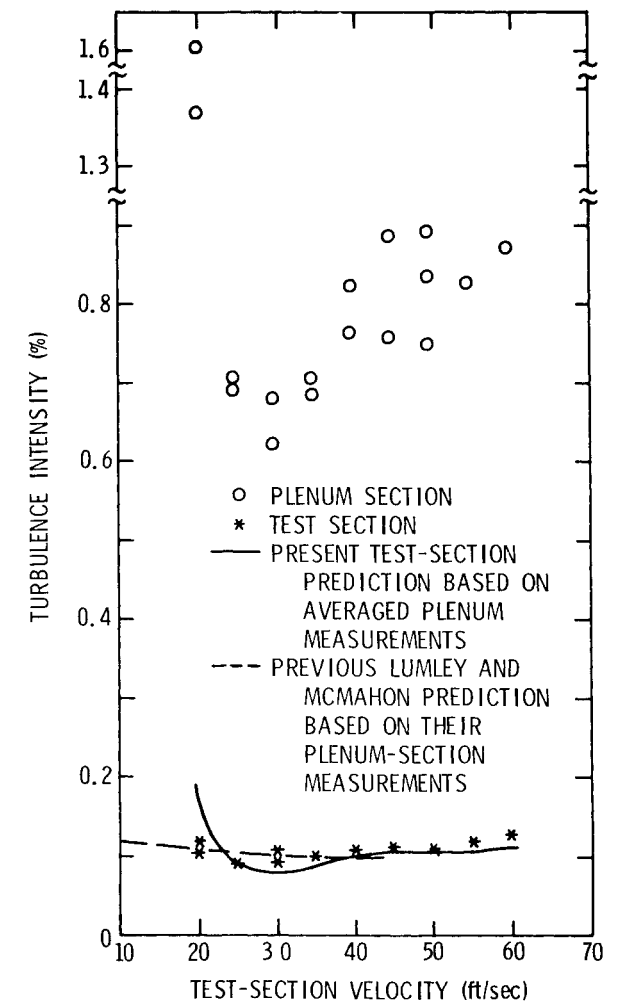

Fig. 6 Measured plenum section and predicted test section turbulence intensity.

measurements were repeated. With the honeycomb installed, the turbulence level drops to around 0.75% in the plenum section. These data agree reasonably well with Lumley and McMahon.[1] Due to the difference in relative axial positioning of the sensors from the honeycomb, McMahon's average data are higher than those of the present measurements.

Figure 5 presents data taken in the test section. With no honeycomb, the average values indicate increased turbulence levels with decreasing impeller pitch angle. The lowest levels were those with 22.5 deg pitch angle; consequently, after the honeycomb was installed, measurements were made only with this pitch angle. As a matter of fact, the impeller is usually set at this pitch angle for normal operation. The addition of the honeycomb lowered the turbulence level by 0.10% to an average 0.11% for the 22.5deg impeller pitch angle.

Following the analysis of Lumley and McMahon,[1] as outlined in the text, the test section turbulence intensity was estimated from measurements made in the plenum section. Figure 6 shows the results of applying Eq. (6) to the average plenum section measurements. In addition, Lumley and McMahon's findings are also presented and compared to measured test section intensity levels. The measured and predicted levels agree quite well; the intensity level was found to be 0.10% for test section velocities of 25 f/s (7.62 m/s) to 60 f/s (18.29 m/s). Even the rise in intensity with increasing speed is reflected in the predicted values.

Although this paper shows the effect a honeycomb has on the axial velocity component in a turbulent flow, Ramjee and Hussain[2] presented extensive data on the effect of the nozzle contraction ratio on freestream turbulence. In addition, in another paper, Hussain and Ramjee[3] also showed the effect of nozzle contraction shapes on turbulent flow. The ratio $(\sqrt{\overline{u^2}}/\bar{U})_T/(\sqrt{\overline{u^2}}/\bar{U})_P$ can be computed from data in Fig. 6 and compared to the results of Ramjee and Hussain.[2] After adjusting the intensity level in the plenum for the additional decay length of 13.89 in. (35.28 cm) to their measuring station, the ratio $(\sqrt{\overline{u^2}}/\bar{U})_T/(\sqrt{\overline{u^2}}/\bar{U})_P$ equals 0.18 at 35 f/s (10.67 m/s), which agrees very well with Ramjee and Hussain's[2] data.

Longitudinal Integral Length Scale

The results of the longitudinal integral length scale measurements are presented in Figs. 7 and 8. In the plenum section, Fig. 7, it appears that the impeller pitch angle does not have much of an effect without a honeycomb. Both 22.5 and 18 deg pitch angles indicate the same results, i.e., that length scales vary from 5.25 in. (13.34 cm) at 20 f/s (6.10 m/s) to around 6.75 in. (17.14 cm) at 60 f/s (18.29 m/s).

In the test section, Fig. 8, it is evident that increasing the pitch angle decreases the length scale. The lower the pitch angle, the more prone the impeller is to cavitation. It seems hard to believe that these large pressure and velocity fluctuations could show themselves after passing through half the tunnel length and two sets of turning vanes. Note that cavitation is noisy and acoustic waves of high intensity do generate velocity fluctuations that can be confused with turbulent fluctuations—$u = p'/\rho c$, where p' is the acoustic pressure amplitude, ρ is the density, and c represents the speed of sound. The lowest length scales are around 0.5 in. (1.27 cm) for the 22.5-deg pitch angle; the average value was 0.71 in. (1.80 cm). With the installation of the honeycomb, the average length scale was slightly reduced to around 0.54 in. (1.37 cm).

A comparison of longitudinal integral scales is made between the no-honeycomb and installed honeycomb condition for the 22.5 deg pitch angle in Fig. 8. In the plenum section, the length scales behind the honeycomb are approximately 4 in. (10.16 cm) smaller than with no honeycomb. There is a $4 \times 4 \times 24$ in. ($10.16 \times 10.16 \times 60.96$ cm) steel honeycomb in the plenum section; without the 0.22 in. (0.56 cm) cell size honeycomb, this large 4 in. (10.16 cm) honeycomb would be the dominant source of flow distur-

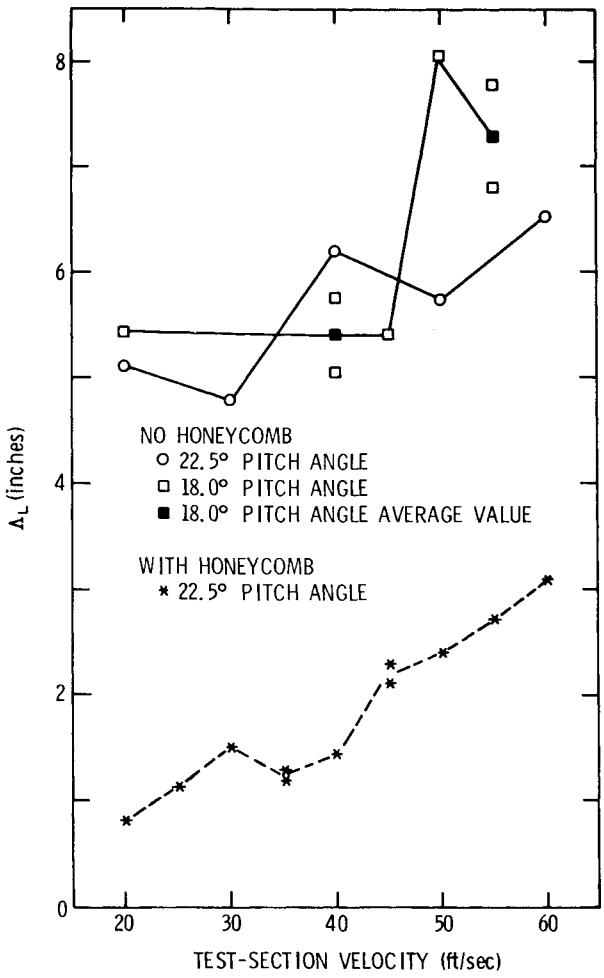

Fig. 7 Longitudinal integral length scales in the plenum section.

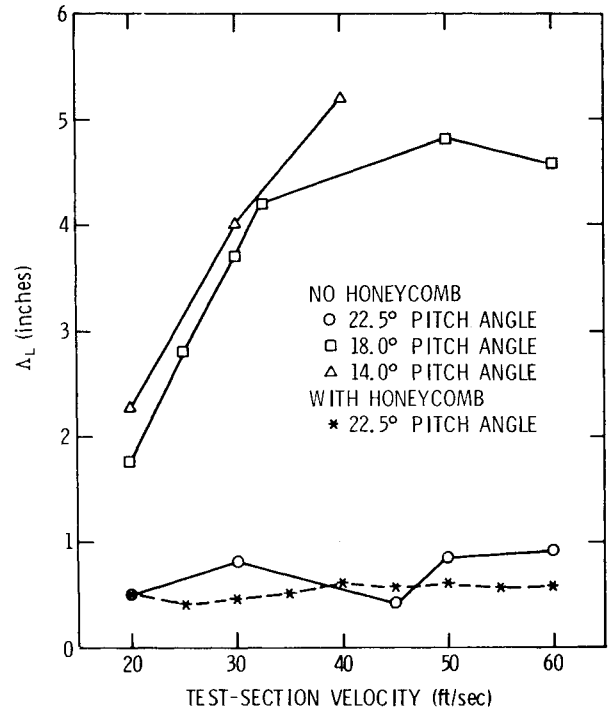

Fig. 8 Longitudinal integral length scales in the test section.

bances. For flows behind the large honeycomb, the length scale should be on the order of 4 in. (10.16 cm), which it is. Downstream in the test section, the integral scales are more nearly the same, only 0.3 in. (0.76 cm) difference. Without the small honeycomb, the scale is approximately 0.8 in. (2.03 cm), while with the honeycomb 0.54 in. (1.37 cm) reflects the scale size.

One-Dimensional Turbulence Energy Spectra

The results of spectral analysis are shown in Figs. 9–12. In all cases, there were no large spikes in the spectral data nor any other abnormalities. Figure 9 shows the turbulent energy spectra at various velocities in the plenum section without the 0.22 in. (0.56 cm) size honeycomb. The frequency has been rendered dimensionless with $d/\bar{U}$ and the energy spectra have been normalized such that

$$\int_0^\infty F\left(\frac{fd}{\bar{U}}\right) d\left(\frac{fd}{\bar{U}}\right) = \overline{u^2}/\bar{U}^2 \tag{8}$$

where F is the normalized spectral density of the kinetic energy per unit mass associated with the longitudinal component of the velocity, d is the cell size of the upstream honeycomb, and $\bar{U}$ is the local axial mean velocity. Spectra are plotted for test section velocities from 20 f/s (6.10 m/s) to 60 f/s (18.29 m/s). The five spectra have the same shape and roughly the same magnitude. It is seen that one of them has a peak at a nondimensional frequency of 1.0, whereas the others have not reached that value. This indicates that the scaling length should be of the order of the large honeycomb scale length of 4.0 in. (10.16 cm) or larger.

The spectra obtained in the plenum with the 0.22 in. (0.56 cm) size honeycomb installed are presented in Fig. 10. Here, the frequency is nondimensionalized by the cell size d of 0.22 in. (0.56 cm). Two things become readily apparent—spectral level and the shifted spectral peaks. First, the peak of the turbulent spectra of the 20 f/s (6.10 m/s) run is approximately one order of magnitude larger than the other test velocities. This did not occur without the honeycomb, in fact, the peak value is higher with the honeycomb. If the Reynolds number based on honeycomb cell diameter is calculated, we find $R_e = \bar{U}d/\nu = 3955$. This value is above the critical Reynolds number of 2300 for pipe flow. However, the low Reynolds number indicates the flow is still in transition from laminar to turbulent, based on a curve of friction factor vs Reynolds number in Shames.[4] Apparently, only some of the cells have fully developed turbulent flow at this low-flow velocity. Shivitz[5] observed an interesting phenomenon in a boundary layer on a body of revolution. He saw a higher turbulence intensity near the end of the transition region than in the region of fully developed turbulent flow. He also observed a shift of the peak spectral energy toward higher frequencies when going from the transition region to the fully developed turbulent region. Notice this also occurs in the spectra in Fig. 10. Evidently the turbulent flow exiting the honeycomb cells was not fully developed. Thus, there might be additional low-frequency energy added to the flow due to these cells still in transition. That is to say, some cells might not be fully developed while other cells nearby were fully developed; thus, these nondeveloped cells would add larger scale eddies to the flow. If this is the case, then the transverse components of the turbulent fluctuations would not be fully suppressed and would be convected downstream. Notice in Fig. 10 that the spectral peaks occur near the same nondimensional frequency for the 30 through 60 f/s (9.14 through 18.29 m/s) runs.

The one-dimensional energy spectra for the test section without the 0.22 in. (0.56 cm) honeycomb are shown in Fig. 11. Here the spectral levels and shapes between the runs are nearly the same as in the plenum section without a honeycomb. You will note that the spectral peaks occur below a nondimensional frequency of 0.05 and a change in slope occurs around 1; comparing this to Fig. 9 for the plenum, there appears to be a slight shift in energy to higher

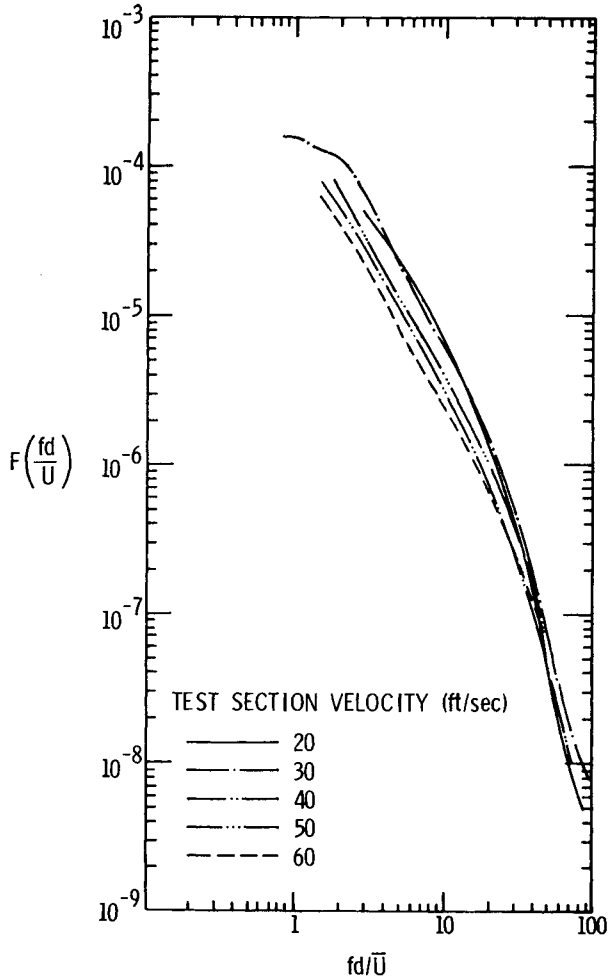

Fig. 9 Turbulence spectra in the plenum section without a honeycomb, $d = 4.0$ in.

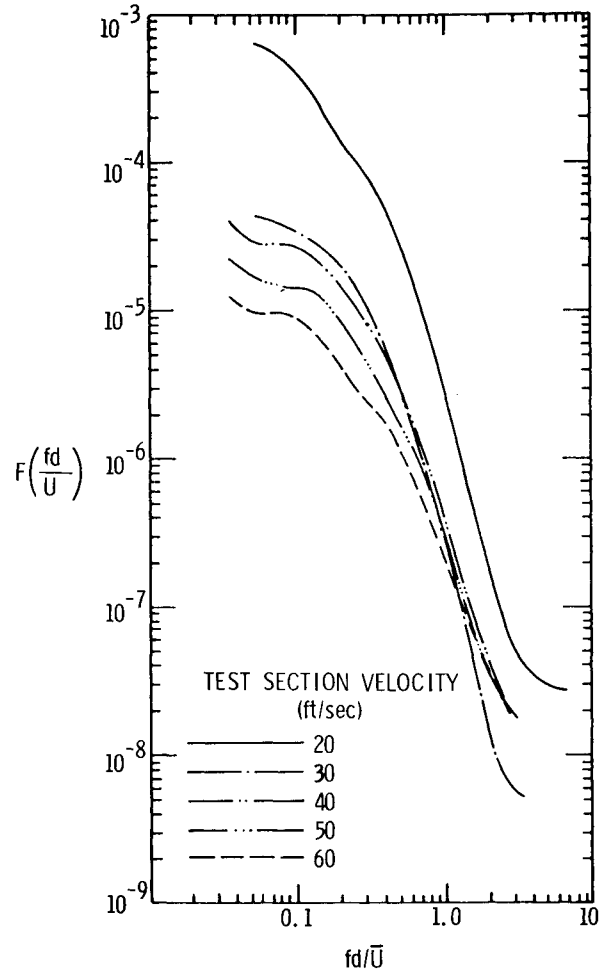

Fig. 10 Turbulence spectra in the plenum section with a honeycomb, $d = 0.22$ in.

frequencies. Also, note that the peak spectral levels in the test section are three orders of magnitude less than in the plenum section. These effects are due to the turbulence decay length and the nozzle contraction ratio.

With the honeycomb installed, the energy spectra in the test section are shown in Fig. 12, where the frequency is nondimensionalized by the honeycomb cell size. Again, the turbulent energy in the 20 f/s (6.10 m/s) run is apparent; the energy level is again an order of magnitude greater than the higher velocity flows. Comparison of the plenum section energy levels to the test section levels is again shown to be three orders of magnitude greater for both the 20 f/s (6.10 m/s) spectrum and the higher speeds.

Table 1 Corrections for a cone film

Parameter comparison ratio	Correction factor or equation
Turbulence intensity	
$\frac{(\sqrt{u^2}/\bar{U})_{x\text{ wire}}}{(\sqrt{u^2}/\bar{U})_{\text{cone}}}$	2.23
Energy spectrum	
$\frac{(F)_{x\text{ wire}}}{(F)_{\text{cone}}}$	$(5.34 - 3.66e^{-0.1(f)}) + 35.82(f/1000) - 45.79(f/1000)^2 + 23.63(f/1000)^3 - 5.19(f/1000)^4 + 0.405(f/1000)^5$

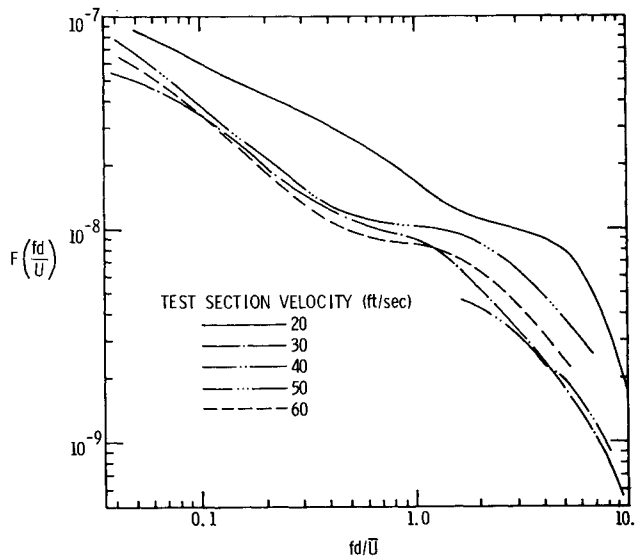

Fig. 11 Turbulence spectra in the test section without a honeycomb, $d = 4.0$ in.

In a recent report by M. F. Young,[6] measurements made with different hot-film probe configurations were compared to those made with an x-array hot-wire probe. His investigation was initiated to find correction factors for the discrepancies between hot-wire and hot-film measurements. He made a careful x-array hot-wire calibration in a two-

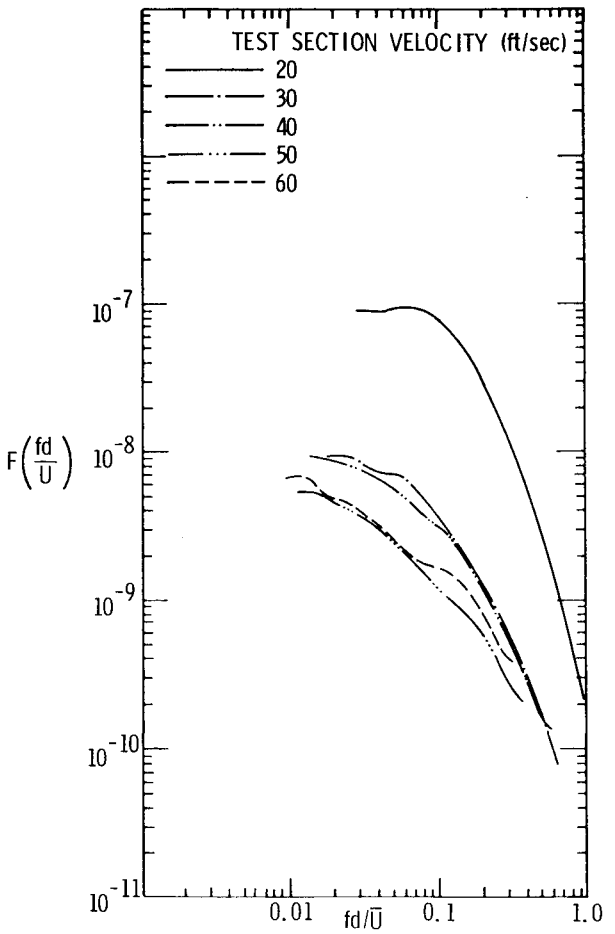

Fig. 12 Turbulence spectra in the test section with a honeycomb, $d = 0.22$ in.

dimensional, steady, incompressible, and fully established turbulent channel flow; both axial and tangential fluctuating velocity components were measured, as well as spectral information. He then repeated his measurements with different hot-film probe configurations.

The need for these correction factors arises from the fact that there is a large heat transfer to the substrate in film probes, whereas in wire type probes most of the heat is convected by the flow. Young then states that the standard hot-wire response equations cannot be applied to hot-film anemometers. Thus, the structure of the hot films yield a frequency-dependent anemometer gain. This then leads to the discrepancies between hot-wire and hot-film measurements.

The correction factors for the turbulence intensity were found to be a constant for each probe design; the correction equation for the spectral analysis was found to be functions of frequency. Young expressed his correction factor as a ratio of the x wire measurements over the film measurements. The corrections for a cone film are given in Table 1, where f denotes frequency in Hz. No data were presented for a parabolic probe. The largest corrections were for the cone film. These correction factors may be applied to data presented in this paper, if Young's results are considered technically valid. However, there are several ways in which Young's results are inconsistent, and it is premature to conclude more than that there may be a correction factor, surely not larger than the preceding. More definitive tests and analyses are presently underway at ARL.

Conclusions

The conclusions drawn from these tests are hereafter given in conjunction with Figs. 6, 8, 10, and 12.

1) The values of the test section turbulence intensity level are shown in Fig. 6. The following comments apply:

a) The measured intensity with the honeycomb has an average value of 0.11% for test section flow velocities between 20 f/s (6.10 m/s) and 60 f/s (18.29 m/s). This is compared to a value of 0.21% measured before installation of the honeycomb.

b) The test section intensity level predicted from measurements made in the plenum indicated a level of 0.10% for test section flow velocities between 25 f/s (7.62 m/s) and 60 f/s (18.29 m/s).

c) The turbulence level at a flow speed of 20 f/s (6.10 m/s) was predicted to be 0.19%, based on measurements in the plenum. This high level is believed to be due to the turbulent flow in the honeycomb cells not being fully developed. Thus, for experimental investigations requiring minimum turbulence levels, the test section flow velocity should be set at a minimum of 25 f/s (7.62 m/s).

d) The measured and predicted intensity values were compared to a previous prediction based on a similar honeycomb and were found to be in excellent agreement.

e) Without the honeycomb installed, the lowest average turbulence intensity corresponded to the tunnel drive impeller pitch angle setting of 22.5 deg. Therefore, it is recommended that this sett ,g be used for experimental tests requiring low turbulence levels.

2) The average longitudinal integral length scale in the test section with the honeycomb installed was found to be 0.54 in. (1.37 cm), as shown in Fig. 8. This was a slight reduction from a value of 0.71 in. (1.80 cm) measured without the honeycomb.

3) The spectral analysis indicated a normal turbulence spectrum; there were no indications of large spikes or other abnormalities in any of the spectral data.

One phenomenon did show up in these data. The peak energy level of the 20 f/s (6.10 m/s) test runs were approximately one order of magnitude larger than higher speed runs both in the plenum and test section, as shown in Figs. 10 and 12. In addition, the peak energy level shifts to higher frequencies at higher tunnel flow speeds. The conclusion from these results and other observations[5] is that at a test section velocity at 20 f/s (6.10 m/s) the turbulent flow through the honeycomb cells is not fully developed. This conclusion is the same as conclusion lc and corroborates the turbulence intensity findings. It is again recommended that this tunnel be operated at flow speeds greater than 25 f/s (7.62 m/s) for minimum turbulence levels.

Acknowledgment

The author would like to thank G. B. Gurney for his help in mounting the hot-film sensor in the 48-in. (1.22-m) water tunnel. This work was performed at the Applied Research Laboratory on the campus of The Pennsylvania State University under contract with the Naval Sea Systems Command.

References

[1] Lumley, J.L. and McMahon, J.F., "Reducing Water Tunnel Turbulence by Means of a Honeycomb," *Transactions of the ASME, Journal of Basic Engineering,* Vol. 89, Dec. 1967, pp. 764-770.

[2] Ramjee, V. and Hussain, A.K.M.F., "Influence of the Axisymmetric Contraction Ratio on Free-Stream Turbulence," *Transactions of the ASME, Journal of Fluids Engineering,* Vol. 98, Sept. 1976, pp. 506-515.

[3] Hussain, A.K.M.F. and Ramjee, V., "Effects of the Axisymmetric Contraction Shape on Incompressible Turbulent Flow," *Transactions of the ASME, Journal of Fluids Engineering,* Vol. 98, March 1976, pp. 58-69.

[4] Shames, I., *Mechanics of Fluids,* McGraw-Hill Book Company, Inc., New York, 1962, pp. 297.

[5] Shivitz, W.F., "An Experimental Investigation of Artificially Induced Transition to Turbulence on a Body of Revolution," ARL Technical Memo., File No. TM 75-178, June 19, 1975.

[6] Young, M.F., "Calibration of Hot-Wires and Hot-Films for Velocity Fluctuations," Rept. TMC-3, Thermosciences Div., Dept. of Mechanical Engineering, Stanford University, Stanford, Calif., March 1976.